

AUTOMATED STAR/GALAXY DISCRIMINATION IN MULTISPECTRAL WIDE-FIELD IMAGES

Jorge de la Calleja

Instituto Nacional de Astrofísica, Óptica y Electrónica, Santa María Tonantzintla, Puebla, México

Olac Fuentes

Computer Science Department, University of Texas at El Paso, El Paso, Texas, U.S.A.

Keywords: Image Analysis, Machine Learning, Imbalanced Datasets.

Abstract: In this paper we present an automated method for classifying astronomical objects in multi-spectral wide-field images. The classification method is divided into three main stages. The first one consists of locating and matching the astronomical objects in the multi-spectral images. In the second stage we create a compact representation of each object applying principal component analysis to the images. In the last stage we classify the astronomical objects using locally weighted linear regression and a novel oversampling algorithm to deal with the unbalance that is inherent to this class of problems. Our experimental results show that our method performs accurate classification using small training sets and in the presence of significant class unbalance.

1 INTRODUCTION

Currently, several multi-band astronomical surveys, such as the Sloan Digital Sky Survey¹, the Two Micron All Sky Survey², and the Digitized Palomar Observatory Sky Survey³, are producing enormous image databases that require automated tools for any kind of analysis. Analyzing wide-field images has been and still is of great importance in astrophysics: from studies of the structure and dynamics of our Galaxy, to galaxy formation and evolution, to the large scale structure of the Universe (Andreon et al., 2000).

Recently, there has been a great deal of interest from astronomers in applying computer vision and pattern recognition techniques to solve astronomical image analysis problems. Examples of these works include classification of galaxies (Bazell and Aha, 2001; DelaCalleja and Fuentes, 2004; Lahav, 1996; Naim et al., 1995; Owens et al., 1996; Storrie-Lombardi et al., 1992), stars (Bailer-Jones et al., 1998), binary stars (Weaver, 2000), star/galaxy discrimination (Andreon, 1999; Mähönen and Hakala,

1995; Philip et al., 2002) and many others. Some works have started using multi-spectral images, for example, Zhang and Zhao used data from the optical, X-ray, and infrared bands to classify active galactic nuclei (AGN), stars, and galaxies, using learning vector quantization, support vector machines and single-layer perceptrons (Zhang and Zhao, 2004).

In general, the first steps in analyzing astronomical images are the detection and classification of the objects in them. This presents significant challenges in the case of multi-spectral images, as astronomical objects have widely varying appearances at different wavelengths. In this work we propose a method to classify astronomical objects in multi-spectral wide-field images in a fully automated manner. This method first locates and matches the objects in the different multi-spectral images. Then, it creates a new representation for each object using its multi-spectral images. After that, it employs principal component analysis to reduce the dimensionality of the data and to find relevant information. Finally, it uses locally weighted linear regression to classify the objects. Since most astronomical problems involve large degrees of class unbalance (for example in our galaxy/star discrimination problem, galaxies outnumber stars by a factor of 10), we also introduce a method to deal the problem of imbalanced data sets.

¹<http://www.sdss.org>

²<http://www.ipac.caltech.edu/2mass>

³<http://dposs.ncsa.uiuc.edu>

de la Calleja J. and Fuentes O. (2007).

AUTOMATED STAR/GALAXY DISCRIMINATION IN MULTISPECTRAL WIDE-FIELD IMAGES.

In *Proceedings of the Second International Conference on Computer Vision Theory and Applications - IU/MTSV*, pages 155-160

Copyright © SciTePress

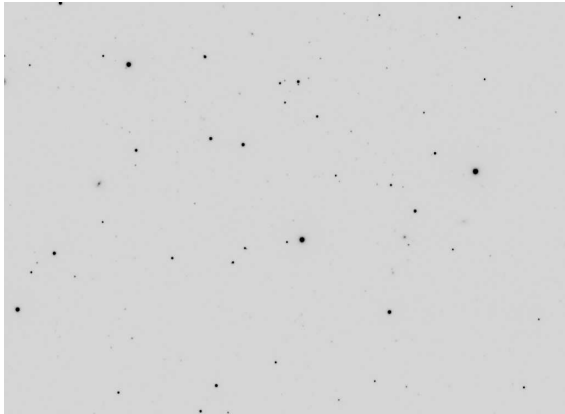


Figure 1: An astronomical wide-field image taken in the infrared band.

The paper is organized as follows: in Section 2 we give a brief introduction about multi-spectral wide-field images in Astronomy. In Section 3 we describe the method for classifying the astronomical objects, including its main three components. Next, in Section 4, we introduce our proposed method for dealing with imbalanced data sets. Section 5 presents experimental results. Some conclusions and directions of future research are presented in Section 6.

2 MULTI-SPECTRAL WIDE-FIELD IMAGES

An astronomical wide-field image (see Figure 1) normally contains from tens to thousands of objects. These objects may be stars, galaxies, nebulae, or quasars, among others. Multi-spectral imaging refers to acquiring several images of the same scene using different spectral bands. The spectral distribution of celestial sources carries essential information about the physical processes that take place in these objects (Nuzillard and Bijaoui, 2000). Generally, multi-spectral images provide more information than a single wavelength one.

The final goal in processing multi-spectral wide-field images is usually to construct catalogues that contain astrometric, geometric, morphological and photometric parameters for each object in the image (Andreon, 1999).

3 THE CLASSIFICATION METHOD

The method we present to classify the astronomical objects is divided into three main stages. The first

one consists of locating and matching the astronomical objects among the multi-spectral images. In the second stage we create a new representation for each object using its multi-spectral images, and also we find a set of features using principal component analysis. Finally, in the last task we classify the astronomical objects using locally weighted linear regression in combination with an oversampling algorithm to deal with the class unbalance inherent to this problem. The following subsections describe in detail these tasks.

3.1 Location and Matching of the Astronomical Objects

First, for each multi-spectral image I we separate the objects from background applying a threshold as follows

$$S(i, j) = \begin{cases} I(i, j), & \text{if } I(i, j) \geq \text{threshold}; \\ 0, & \text{otherwise.} \end{cases} \quad (1)$$

where S is the segmented image, and (i, j) represent a position in the image.

Then, we locate the astronomical objects in the segmented images. We can locate an object by the coordinates (x_1, y_1, x_2, y_2) of the bounding rectangle that encloses it. Our algorithm for locating objects is based on the *flood-fill* algorithm (Hearn and Baker, 1997). The purpose of flood fill is to color an entire area of connected pixels with the same color.

We assume that all the pixels that appear different from the background correspond to astronomical objects. Thus, our algorithm proceeds as follows: We examine every location in the image, then when we find a pixel different from the background, we search its neighbors, i.e. we search its neighbors in the right, left, up and down directions, and mark these pixels. We store the positions of these neighbors to examine again their neighbors. When we find a left neighbor and its position x_1 is smaller than the previous one, we will change it. We do the same for y_1 , x_2 and y_2 , but considering up, right and down, respectively. This process is repeated until the image is fully examined. In the end we will have located each object in each of the multi-spectral images by its coordinates (x_1, y_1, x_2, y_2) . In Table 1 we outline the algorithm to locate objects, and in Figure 2 we show an example of location of objects.

We select some of the located objects according to their size, i.e. if the objects are larger than a threshold we will select them. We do this selection process because many objects are very small, two or three pixels of size.

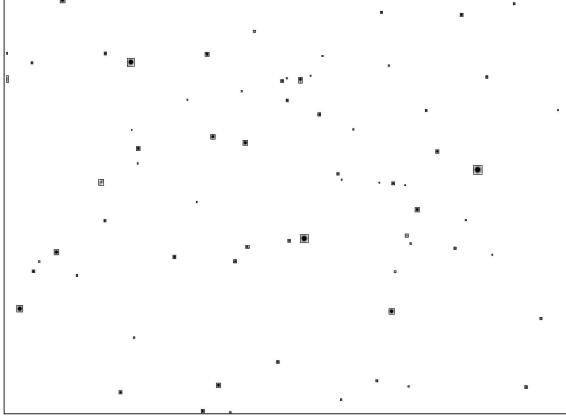


Figure 2: The located objects are marked by a rectangle.

Table 1: The algorithm to locate the astronomical objects.

S is the segmented image, with r rows and c columns
 N is the set of neighbors, initially empty
For $i = 1$ to r
 For $j = 1$ to c
 If $S(i, j) \neq \text{background}$ and is not marked
 - $x_1 = j$
 - $y_1 = i$
 - $x_2 = j$
 - $y_2 = i$
 - $N = (i, j)$
 while $N \neq \emptyset$ do:
 - Find the right, left, up
 and down neighbors of (i, j)
 - Add to N the neighbors of (i, j)
 - if it is necessary
 Modify (x_1, y_1, x_2, y_2)
 - Mark $S(i, j)$ and its neighbors
 - Erase marked neighbors in N
 endwhile
 endfor
 endfor

Most of the time a single object does not appear in exactly the same location in the different multi-spectral images. This can be due to slight misalignments in the imaging system, tracking errors in the telescope, or actual differences in appearance of the object at different wavelengths. Also, these objects may appear in different sizes or they may not even appear at all at some wavelengths. Therefore, we have to devise an algorithm to robustly identify the same object in the different multi-spectral images.

The idea of our algorithm to match objects is the following: We search the largest object among the multi-spectral images. Then, we use its coordinates (x_1, y_1, x_2, y_2) to find the same object, but in the other images. Almost always the object may not appear exactly in the same position, then we use the Euclidean distance to match the closest object to our interest point. Sometimes we may not match any object be-

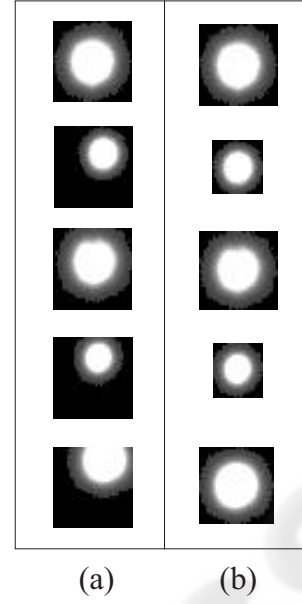


Figure 3: Column (a) shows an object in the different multi-spectral images. We can see that this one is not located in the same position. Column (b) shows the same object after matching.

cause in the images may appear only black pixels; in these cases we assign as match point the location of the largest object. This process is repeated until all the objects have been matched. Because we match an object in five multi-spectral images, we will have five representations of the same object. Table 2 summarizes our algorithm to match objects and Figure 3 shows an example of matching.

Table 2: The algorithm to match the astronomical objects.

Γ is the set of multi-spectral images
while Γ contains objects to match do:
 - Find G , the largest object in Γ
 - Obtain p_g , the coordinate where G was found
 - Obtain r_g , the region that encloses G
 - Obtain Γ_g , the image where G was found
 - $Q = \Gamma - \Gamma_g$
 - Search G in Q
 - Let $q = (x_c, y_r)$ be the coordinates
 of the objects in Q
 - Find the closest objects to p_g
 with q using the Euclidean distance
 - $\Delta =$ the matched objects
 - Erase the matched objects in Γ
endwhile

3.2 Extracting Features

Once we have located and matched the astronomical objects in the multi-spectral images, we crop each object in the original image set to create our data set.

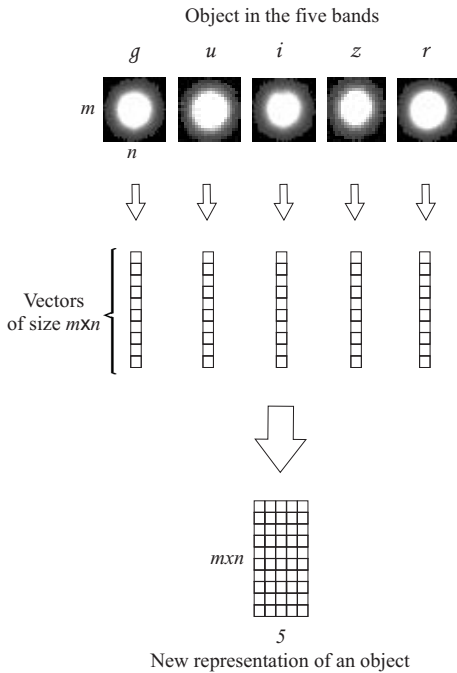


Figure 4: Process to create a new object representation.

Again, we use the coordinates (x_1, y_1, x_2, y_2) of each object to crop it.

Each object has five representations, according to the different bands u, g, r, i and z . Each $m \times n$ image at each wavelength is converted into a vector of length mn , then, these vectors are concatenated to create a matrix of size of $m \times n \times 5$, i.e. the size of the vector by the number of multi-spectral representations. In figure 4 we show the process of creating this new representation.

Because we have a large data set, we use principal component analysis (PCA) to reduce its dimensionality and also to find features (principal components) that permit us to classify the astronomical objects. Details about PCA can be found in (Turk and Pentland, 1991).

3.3 Classifying Objects

Finally, we use locally weighted linear regression (LWLR) to classify the astronomical objects. This machine learning algorithm takes as input parameters the projection of the new representation of the objects onto a few set of principal components. Next, we briefly describe this method.

3.3.1 Locally Weighted Linear Regression

Locally-weighted regression belongs to the family of instance-based learning methods. These kinds of al-

gorithms simply store all training examples, and when they have to classify new instances, they find similar examples to them. In this work we use a linear model around the query point to approximate the target function.

Given a query point x_q , to predict its output parameters y_q , we assign to each example in the training set a weight given by the inverse of the distance from the training point to the query point:

$$w_i = \frac{1}{|x_q - x_i|} \quad (2)$$

Let W , the weight matrix, be a diagonal matrix with entries w_1, \dots, w_n . Let X be a matrix whose rows are the vectors x_1, \dots, x_n , the input parameters of the examples in the training set, with the addition of a "1" in the last column. Let Y be a matrix whose rows are the vectors y_1, \dots, y_n , the output parameters of the examples in the training set. Then the weighted training data are given by $Z = WX$ and the weighted target function is $V = WY$. Then we use the estimator for the target function defined as:

$$y_q = x_q^T Z^* V \quad (3)$$

where Z^* is the pseudoinverse of Z .

4 THE METHOD TO DEAL IMBALANCED DATA SETS

The class imbalance problem occurs when there are many more examples of some classes than others, such as in our case, where we have more examples of stars than galaxies. Two main approaches have been used in machine learning to deal with class imbalance. The first consists of assigning distinct costs to training examples, weighting more heavily those in the minority class (Pazzani et al., 1994; Domingos, 1999). The second approach is to re-sample the original dataset, either by over-sampling the minority class and/or under-sampling the majority class (Japkowicz, 2000; Kubat and Matwin, 1997; Chawla et al., 2002).

Our method follows the second approach, and is similar to the SMOTE (Chawla et al., 2002) algorithm, i.e. the minority class is over-sampled by taking each minority class sample and adding synthetic examples in the original data. The purpose of augmenting the minority class is to create a balanced data set, which helps to improve results in the classification task.

Our method generates the synthetic examples as follows: First we separate positive and negative examples from the original data set, then we find the n

Table 3: The algorithm to create new examples.

D is the original data set
 N is the set of negative examples
 $P = D - N$
for each example E in P

- Find the n closest examples to E using the weighted distance
- Obtain A , the average of n
- $\delta = E - A$
- $\eta = E + \delta * \sigma(0, 1)$

Add η to D

endfor

closest examples to each positive (minority) example using the weighted distance and taking into account only the positive data set. Then we average these n closest instances, take the difference between each minority example (under consideration) and the average instance, multiply this difference by a random number between 0 and 1, and add it to the original data set. Table 4 outlines our oversampling algorithm.

5 EXPERIMENTAL RESULTS

We tested our method using images taken in five wavelengths: u , g , r , i and z , i.e. one in ultraviolet, one using the green filter, one using the red filter, and two infrared, respectively. These images are of size of 1489×2048 pixels and were obtained from the Sloan Digital Sky Survey. We used two data sets, the first one (DB1) contained 62 stars and 7 galaxies, and the second one (DB2) had 141 stars and 28 galaxies. These objects were labeled by hand, i.e. we examine each image and assign a label to each object.

We used 3 principal components that represent about 90% of the original information in the data sets. We implemented locally weighted linear regression and the over-sampling method in MatlabTM.

In all the experiments reported here we used 10-fold cross-validation. Also, we vary the amount for over-sampling from 0% to 1000%. The results we show later correspond to the average of five runs.

We evaluated our method using two metrics: precision and recall. This metrics can be defined as follows:

$$Recall = TP / (TP + FN) \quad (4)$$

$$Precision = TP / (TP + FP) \quad (5)$$

Where TP denotes the number of positive examples that are classified correctly, while FN and FP

Table 4: The table below show the results for the first data set (DB1) using different amount for over-sampling.

| | 0% | 100% | 200% | 400% | 1000% |
|-----------|------|------|------|------|-------|
| Recall | .343 | .400 | .343 | .485 | .542 |
| Precision | .486 | .530 | .500 | .474 | .607 |

Table 5: The table below show the results for the second data set (DB2) using different amount for over-sampling.

| | 0% | 100% | 200% | 400% | 1000% |
|-----------|------|------|------|------|-------|
| Recall | .692 | .757 | .750 | .742 | .742 |
| Precision | .740 | .789 | .774 | .771 | .667 |

denote the number of misclassified positive and negative examples, respectively.

In Table 4 we show the results for the first data set (DB1). We can observe that the best results are obtained when we use 1000% for over-sampling, i.e. .542 and .607 for recall and precision, respectively. In Table 5 we show the results for the second data set (DB2). Here we can see that better results are obtained than using DB1. This may be due to the fact that we have more examples to train our classifier. Also, the best results were obtained using only 100% for over-sampling, with .757 for recall and .789 for precision.

6 CONCLUSION

We have presented a method for classifying astronomical objects in multi-spectral wide-field images in a fully automated manner. Also, we introduced a method to deal with imbalanced data sets that permits to improve classification results. Our results are comparable with the best reported in the literature, but we are using significantly smaller training sets, thus better results should be expected when we experiment with larger data sets. Current and future work includes: testing the method for classifying more types of astronomical objects, using larger data sets, and testing the oversampling method on standardized data sets.

ACKNOWLEDGEMENTS

The first author wants to thank CONACyT for supporting this research under grant 166596.

REFERENCES

- Andreon, S. (1999). Neural nets and star/galaxy separation in wide field astronomical images. In *Proceedings of International Joint Conference on Neural Networks*.
- Andreon, S., Gargiulo, G., Longo, G., Tagliaferri, R., and Campuano, N. (2000). Wide field imaging - i. applications of neural networks to object detection and star/galaxy classification. *Monthly Notices of the Royal Astronomical Society*, 319:700–716.
- Bailer-Jones, C., C.A.L., Irwin, M., and von Hippel, T. (1998). Automated classification of stellar spectra. ii: Two-dimensional classification with neural networks and principal components analysis. *Monthly Notices of the Royal Astronomical Society*, 298:361.
- Bazell, D. and Aha, D. (2001). Ensembles of classifiers for morphological galaxy classification. *The Astrophysical Journal*, 548:219–233.
- Chawla, N., Bowyer, K., Hall, L., and Kegelmeyer, P. (2002). Smote: Synthetic minority over-sampling technique. *Journal of Artificial Intelligence Research*, 16:321–357.
- DelaCalleja, J. and Fuentes, O. (2004). Machine learning and image analysis for morphological galaxy classification. *Monthly Notices of the Royal Astronomical Society*, 349:87–93.
- Domingos, P. (1999). Metacost: A general method for making classifiers cost-sensitive. In *Proceedings of the 5th International Conference on Knowledge Discovery and Data Mining*, pages 155–164.
- Hearn and Baker (1997). *Computer Graphics*. Prentice Hall, 2nd. edition.
- Japkowicz, N. (2000). The class imbalance problem: Significance and strategies. In *Proceedings of the 2000 International Conference on Artificial Intelligence (IC-AI'2000): Special Track on Inductive Learning*, pages 111–117.
- Kubat, M. and Matwin, S. (1997). Addressing the curse of imbalanced training sets: One sided selection. In *Proceedings of the Fourteenth International Conference on Machine Learning*, pages 179–186.
- Lahav, O. (1996). Artificial neural networks as a tool for galaxy classification. In *Proceedings in Data Analysis in Astronomy*.
- Mäihönen, P. and Hakala, P. (1995). Automated source classification using a kohonen network. *The Astrophysical Journal*, 452:L77–L80.
- Naim, A., Lahav, O., Sodr , L., Jr, and Storrie-Lombardi, M. (1995). Automated morphological classification of apm galaxies by supervised artificial neural networks. *Monthly Notices of the Royal Astronomical Society*, 275:567.
- Nuzillard, D. and Bijaoui, A. (2000). Blind source separation and analysis of multispectral astronomical images. *Astronomy and Astrophysics*, 147:129.
- Owens, E., Griffiths, R., and Ratnatunga, K. (1996). Using oblique decision trees for the morphological classification of galaxies. *Monthly Notices of the Royal Astronomical Society*, 281:153.
- Pazzani, M., Merz, C., Murphy, P., Ali, K., Hume, T., and Brunk, C. (1994). Reducing misclassification costs. In *Proceedings of the Eleventh International Conference on Machine Learning*, pages 217–225.
- Philip, N., Wadadekar, Y., Kembhavi, A., and Joseph, K. (2002). A difference boosting neural network for automated star-galaxy classification. *Astronomy and Astrophysics*, 385:1119–1126.
- Storrie-Lombardi, M., Lahav, O., Sodr , L., Jr, and Storrie-Lombardie, L. (1992). Morphological classification of galaxies by artificial neural networks. *Monthly Notices of the Royal Astronomical Society*, 259:8.
- Turk, M. and Pentland, A. (1991). Eigenfaces for recognition. *Journal of Cognitive Neuroscience*, 3(1):71–86.
- Weaver, B. (2000). Spectral classification of unresolved binary stars with artificial neural networks. *The Astrophysical Journal*, 541:298–305.
- Zhang, Y. and Zhao, Y. (2004). Automated clustering algorithms for classification of astronomical objects. *The Astrophysical Journal*, 422:1113–1121.